Phase diagram of the Holstein-Kondo lattice model at half filling

Reza Nourafkan
Department of Physics, Sharif University of Technology, P.O. Box 11155-9161, Tehran, Iran

Nasser Nafari
Institute for Studies in Theoretical Physics and Mathematics, P.O. Box 19395-5531, Tehran, Iran

(Received 31 August 2008; revised manuscript received 22 January 2009; published 26 February 2009)

We study the Kondo lattice model which is modified by the Holstein term, involving both the Kondo exchange coupling and the electron-phonon coupling constants, characterized by J and g, respectively. The model is solved by employing the dynamical mean-field theory in conjunction with the exact diagonalization technique. A zero-temperature phase diagram of symmetry unbroken states at half filling is mapped out which exhibits an interplay between the two interactions and accounts for both spin and charge fluctuations. When the Kondo exchange coupling is dominant the system is in the Kondo insulator state. Increasing g for small values of J leads to a Kondo insulator-metal transition. Upon further enhancement of g a transition to the bipolaronic insulating phase takes place. Also a small region with non-Fermi-liquid behavior is found near the Kondo insulator-metal transition.

DOI: 10.1103/PhysRevB.79.075122 PACS number(s): 71.10.Fd, 71.30.+h, 71.38.−k

I. INTRODUCTION

There has been continued interest in a class of compounds called heavy-fermion semiconductors, which exhibit a spin and a charge gap at low temperatures typically ranging from 1 to 100 meV.[1,2] In contrast to the ordinary band insulators, these two gaps are different, indicating a separation of the spin and charge degrees of freedom brought about by correlation effects. The gap formation in heavy-fermion semiconductors is attributed to the renormalized hybridization between a broadband of conduction electrons and a nearly flat band of strongly correlated f electrons.

The Kondo lattice model (KLM) at half filling is considered to be a good starting point for investigating the properties of the heavy-fermion semiconductors. In this model, at each lattice site a local moment interacts with the spin of a conduction electron and, thus, results in complex correlation effects between them. In fact, a conduction and a localized electron with antiparallel spins undergo a spin-flip process, causing itinerant electrons to leave a trace of their spin exchange at each localized spin site. As a result, the direction of a localized spin is affected by the history of the electrons passing through it. There are similar correlation effects in the periodic Anderson model due to the dynamical aspects of the localized electrons.

Experiments involving the Kondo insulators at high magnetic fields indicate the closure of the Kondo insulating gap, exemplifying a transition from the Kondo insulator to a correlated metal.[3,4] It is expected that the electron-phonon (e-ph) interaction leads to similar results. Many experiments suggest that the e-ph effects are important in describing a number of observations such as the existence of an unusual phonon softening in the Kondo lattice, $CeCu_2$, which is indicative of coupling between electrons and phonons.[5] It is believed that the coupling between phonon modes and the Kondo effect could manifest new material properties, such as non-Fermi-liquid behavior and unconventional superconductivity.[6–8] Furthermore, the lattice plays an important role in some heavy-fermion compounds, such as $Yb_{14}MnSb_{11}$, called 14-1-11, where various properties can be altered through isoelectronic substitutions.[9] In particular, Burch *et al.*,[9] motivated by the coexistence of the magnetic and heavy-fermion properties in these compounds, set out to study the Kondo-phonon coupling experimentally. Their ultrafast optical experiments showed that the relaxation time and amplitude of the photoinduced response increase significantly at low temperatures. These authors, consequently, concluded that such low-temperature behavior is an indication of a charge gap and of the softening of phonons. Our theoretical results are consistent with these experimental findings. Our calculations show that for small g values the imaginary part of the self-energies diverges as $\omega_n \to 0$, which confirms the presence of a charge gap. Moreover, the calculated phonon spectral function shows a considerable phonon softening for g values close to the transition point from the metallic phase to the insulating bipolaronic phase.

Even fewer studies have been devoted to the role played by lattice vibrations in these compounds. The role of the lattice vibrations is not trivial, but if, on general grounds, the minimal effect of e-ph coupling is a phonon-retarded attraction between conduction electrons with opposite spins, then the spin excitation has a gap, while the charge excitation, depending on the strength of the e-ph coupling, can be either gapful or gapless. Therefore, there arises a competition between the spin and charge fluctuations whose behavior is determined, on one hand, by the relative strength of the Kondo exchange between the conduction electrons and the localized moments and, on the other hand, by the conduction electron-phonon coupling, leading to a complicated phase diagram. It is the goal of this paper to investigate the dynamical competition between the e-ph and Kondo interactions.

This paper is organized as follows. In Sec. II we present the Holstein-Kondo lattice model (H-KLM) which is solved by employing the dynamical mean-field theory (DMFT) in conjunction with the exact diagonalization (ED) technique. The results for the phase diagram of the system and phonon

spectral function are presented in Sec. III. Finally, in Sec. IV, we talk about the concluding remarks.

II. MODEL IN DMFT SCHEME

A natural way of incorporating the e-ph coupling in the KLM is to add the Holstein coupling term to its Hamiltonian. In the Holstein coupling the phonon variables are coupled to the local density of the conduction electrons. In this paper, we will present the zero-temperature phase diagram of the H-KLM at half filling. The focus is on the transition between the unbroken-symmetry ground state as the e-ph and Kondo interactions parameters, J and g, are varied.

The H-KLM Hamiltonian is defined by

$$H = -t\sum_{\langle i,j\rangle\sigma}(c_{i\sigma}^{\dagger}c_{j\sigma} + \text{c.c.}) + \frac{J}{2}\sum_{i,\alpha\beta}\boldsymbol{S}_i\cdot(c_{i\sigma}^{\dagger}\boldsymbol{\sigma}_{\alpha\beta}c_{i\sigma}) + g\sum_i(n_i-1)(b_i^{\dagger}+b_i) + \Omega_0\sum_i b_i^{\dagger}b_i, \tag{1}$$

where $c_{i\sigma}$ ($c_{i\sigma}^{\dagger}$) and b_i ($b_i^{\dagger}$) are, respectively, destruction (creation) operators for itinerant electrons with spin σ and local vibrons of frequency Ω_0 on site i, n_i is the electron density on site i, $\boldsymbol{S}_i$ is the spin operator for the localized spin on site i, $\boldsymbol{\sigma}$ is a pseudovector represented by Pauli spin matrices, t stands for the itinerant electrons' hopping matrix elements between the nearest-neighbor sites, J is the coupling strength between itinerant electrons and localized spins, and g denotes the electron-phonon coupling. We do not consider the Coulomb repulsion term between itinerant electrons because it tends to suppress the double occupation of sites, and in our model the exchange coupling J already does the same thing.

Our calculations are based on the dynamical mean-field theory,[10] a powerful nonperturbative tool for studying the properties of strongly correlated systems, which allows us to treat, on equal footing, the two kinds of interactions present in our model. This technique, which becomes exact in the limit of infinite coordination number, reduces the full lattice many-body problem to a local impurity embedded in a self-consistent effective bath of free electrons, mimicking the effect of the full lattice on the local site. Our model (1) becomes a Holstein-Kondo impurity model,

$$H = -\sum_{\mathbf{k}\sigma}V_{\mathbf{k}}(c_{0\sigma}^{\dagger}a_{\mathbf{k}\sigma} + \text{c.c.}) + \sum_{\mathbf{k}\sigma}\epsilon_{\mathbf{k}}a_{\mathbf{k}\sigma}^{\dagger}a_{\mathbf{k}\sigma} + \frac{J}{2}\sum_{\alpha\beta}\boldsymbol{S}_0\cdot(c_{0\sigma}^{\dagger}\boldsymbol{\sigma}_{\alpha\beta}c_{0\sigma}) + g(n_0-1)(b^{\dagger}+b) + \Omega_0 b^{\dagger}b, \tag{2}$$

where $\epsilon_{\mathbf{k}}$ and $V_{\mathbf{k}}$ are the energies and the hybridization parameters of the effective impurity model (bath parameters) and the phonons are defined only on the impurity site 0, which is a representative site of the lattice. A self-consistency condition links effective impurity model (2) to the original lattice problem. Adopting a semicircular density of states (DOS) $\rho_0(\epsilon)=(2/\pi D)\sqrt{D^2-\epsilon^2}$ of the noninteracting system, corresponding to a Bethe lattice with the half bandwidth D, the self-consistency relation imposed on the DMFT solution is given by

$$\frac{D^2}{4}G(i\omega_n) = \sum_k \frac{V_{\mathbf{k}}^2}{i\omega_n - \epsilon_{\mathbf{k}}}. \tag{3}$$

We use the ED technique to solve the effective impurity model.[11] This solver allows us to access the ground-state properties of the system with a finite-energy resolution. The ED technique consists of restricting the sum in Eq. (3) to a small number of levels (n_s) and, moreover, it truncates the infinite phonon Hilbert space, allowing for a maximum number of excited phonons N_{ph}. The ground state and the Green's function of our discretized model are determined via the Lanczos procedure, and the self-consistency equation in turn allows us to derive a different free impurity Green's function $\mathcal{G}_{\text{imp}}^0(i\omega_n)$. A different set of bath parameters is obtained by minimizing the following cost function:

$$\chi^2 = \frac{1}{n_{\max}+1}\sum_{n=0}^{n_{\max}}|\mathcal{G}_{\text{imp}}^0(i\omega_n)^{-1} - \mathcal{G}_{n_s}^0(i\omega_n)^{-1}|, \tag{4}$$

where $\mathcal{G}_{n_s}^0(i\omega_n)$ is the free impurity Green's function of the n_s site. The fit of $\mathcal{G}_{\text{imp}}^0(i\omega_n)$ is performed on the imaginary axis $i\omega_n = i(2n+1)\pi/\tilde{\beta}$ with a fictitious inverse temperature $\tilde{\beta}$, which introduces a low-energy cutoff.[12] The process is iterated until convergence is reached. The value of N_{ph} has to be chosen with special care in strong coupling, where phonon excitations are energetically convenient. Here we use N_{ph} ranging from 30 to 50. As far as the discretization of the bath is concerned, the convergence of self-energy as a function of Matsubara frequencies is exponentially fast and $n_s \sim 8-9$ is enough to obtain converged results.[13] In all the calculations presented here the convergence of both truncations has been checked by repeating the calculations for larger values of n_s and N_{ph}.

In the KLM, the polarization cloud of conduction electrons produced by a local moment may be felt by another local moment, when the coupling strength is weak. This provides the mechanism for the Ruderman-Kittel-Kasuya-Yosida (RKKY) interaction. On the other hand, the same polarization cloud can also form a singlet bound state with the local moment.[14] The RKKY interaction leads to a long-range-ordered antiferromagnetic (AF) phase and the Kondo effect screening leads to short-range spin correlations due to the formation of coherent Kondo spin singlets. There is a quantum phase transition between the two limiting phases upon changing the parameters of the model.[15] Here, following the work of Werner and Millis,[16] by symmetrization of the Green's function, we have suppressed the AF phase caused by RKKY interaction in the weak-coupling limit.

III. RESULTS

Figure 1 shows the $T=0$ phase diagram of the half-filled H-KLM in the parameter space of J and g with $D=2t=2$ and $\Omega_0/t=0.2$. All types of long-range orders are excluded. Three different phases are distinguished: metallic phase and the bipolaronic and Kondo insulating phases. In what follows, a detailed discussion of the phase diagram of these systems will be presented. The Kondo lattice model ($g=0$) and Holstein model ($J=0$), which are special limiting cases of the

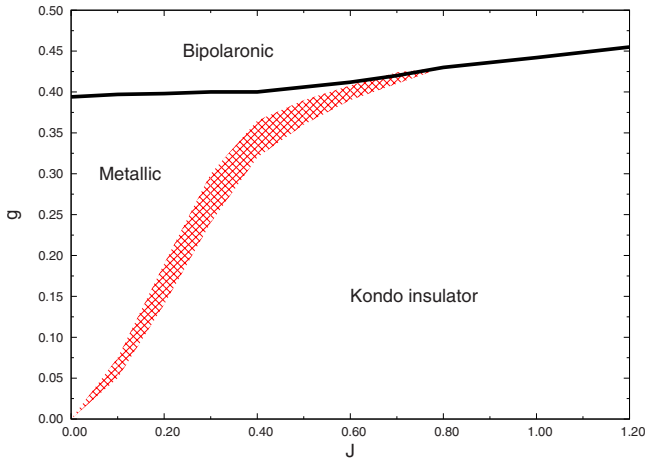

FIG. 1. (Color online) Zero-temperature phase diagram of the unbroken-symmetry Holstein-Kondo lattice model at half filling. The model shows three different phases: metallic, bipolaronic, and Kondo insulating phases. The narrow shaded region with non-Fermi-liquid character is seen near the Kondo insulator-metal transition.

H-KLM, have been extensively studied using the DMFT. The ground state of the KLM is the Kondo insulating phase with a spin and a charge gap for all J values.[17] For the Holstein model, the ground state is metallic. The metallic phase is found to be a Fermi liquid, in the sense that the Luttinger sum rule $\rho(0)=\rho_0(0)$ for the spectral function $\rho(\omega)=-\mathrm{Im}\, G(\omega+i0^+)/\pi$ or, equally stated, the limit of $\mathrm{Im}\, G(i\omega_n)\to -1$ as $\omega_n\to 0$ is satisfied (ω_n is the Matsubara frequency). Upon increasing g, the conduction electrons lose their mobility, eventually acquiring polaronic character, in which the presence of an electron is associated with a finite lattice distortion. Also, the same e-ph coupling can cause any two polarons to attract and form a bound pair in real space, called a bipolaron.[18] In the absence of pair hopping, the bipolaron formation would cause the system to undergo a first-order metal to bipolaronic insulating phase transition at the critical coupling g_c.[19,20] Meyer *et al.*[21] reported that there is a coexistence region near g_c, which is reduced as the phonon frequency Ω_0 is decreased and disappears for $\Omega_0 \leq 0.10D$. The bipolaron formation may be accommodated by reconstructing the system into a phase-separated state[22] or a charge-ordered state in which the doubly occupied and empty sites alternate in real space.[23]

At small fixed J values, with increasing e-ph coupling, a continuous transition to a metallic state occurs at a critical coupling $g_{c1}(J)$, whose value increases with increasing J. This behavior is physically expected. An increase in J leads to a larger insulating gap, and this, in turn, leads to the suppression of the charge fluctuations which would otherwise couple to phonons. As a result a transition to the metallic state occurs at larger e-ph coupling. We also find that the metallic phase near g_{c1} shows non-Fermi-liquid character. Further increase in g causes a metal-bipolaronic phase transition taking place at a critical coupling g_{c2}. As can be distinguished, a Holstein coupling is weakly affected by exchange coupling between conduction electrons with local spins. The metallic state becomes more correlated as g or J is

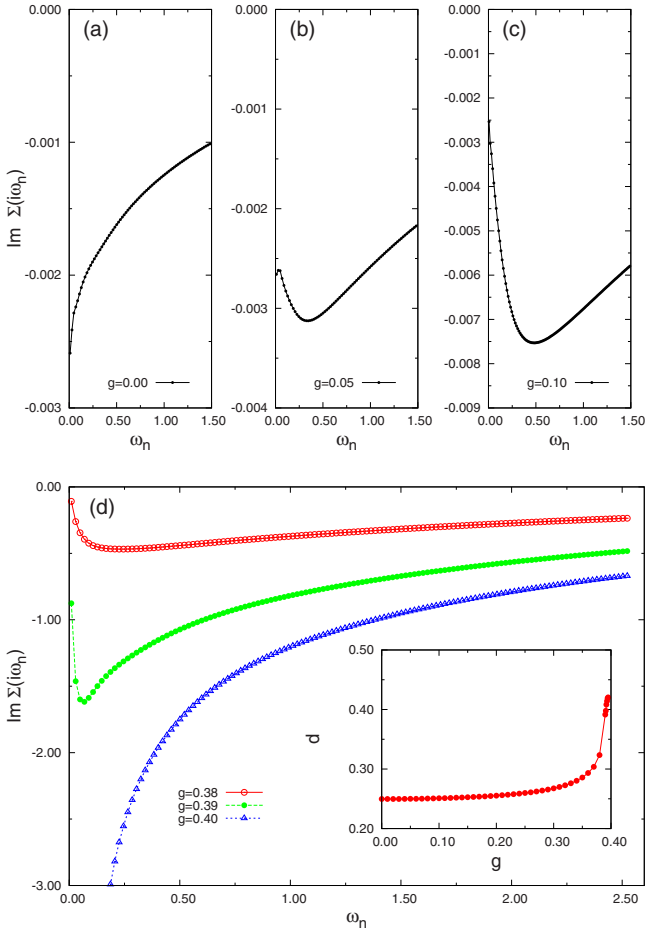

FIG. 2. (Color online) Imaginary part of electron self-energy, $\mathrm{Im}\,\Sigma(i\omega_n)$, obtained at different values of g in the vicinity of both phase transitions, with fixed $J=0.1$. Panels (a)–(c): $\mathrm{Im}\,\Sigma(i\omega_n)$ in the vicinity of the transition from the Kondo insulator state to the metallic state. Changing the $\mathrm{Im}\,\Sigma(i\omega_n)$ behavior as $\omega_n\to 0$ from diverging to extrapolating to zero shows the insulator-metallic phase transition. Panel (d): $\mathrm{Im}\,\Sigma(i\omega_n)$ in the vicinity of the transition from the metallic state to the bipolaronic state. Inset: the double occupancy $d=\langle n_\uparrow n_\downarrow\rangle$ as a function of g. The transition from the metallic state to the bipolaronic state is clearly visible by observing when the double occupancy's jump to $\approx 1/2$ begins to set in.

increased. This is reflected in the decreasing behavior of the quasiparticle weight $z=1/[1-\mathrm{Im}\,\Sigma(i\omega_0)/\omega_0]$ when g or J is increased. (The graph for the quasiparticle weight is not presented in here.)

Figure 2 shows the imaginary part of the electron self-energy, $\mathrm{Im}\,\Sigma(i\omega_n)$, for $J=0.1$ and several values of g in the vicinity of both phase transitions. For small g values, the imaginary part of the self-energies diverges as $\omega_n\to 0$, indicating the presence of a charge gap [see panel (a)]. Increasing g causes the system to change its phase from an insulator to a bad metal in the sense that its self-energy extrapolates to a finite value $\mathrm{Im}\,\Sigma(i0^+)\equiv\Gamma(J)\neq 0$ for $g\geq g_{c1}$ [panel (b)]. Hence, a finite lifetime is found at the Fermi level for a narrow range of e-ph couplings near g_{c1}, indicating that well-defined quasiparticles do not exist in this range. The violation of the Luttinger sum rule in this region is also seen from $\mathrm{Im}\,G(i\omega_n)$, which tends to a negative constant ($c<0$) in the

limit of $\omega_n \to 0$, with $|c| < \pi\rho_0(0) = 1$. Although the discreteness of the spectra obtained in the exact diagonalization technique does not allow us to unambiguously identify the non-Fermi-liquid region, we believe that the spectral function at $g=0$ displays a narrow insulating gap, whose width is proportional to the value of J, with two peaks on each side. For a fixed J, increasing g causes the low-energy spectrum to widen and it is also suppressed. If these peaks overlap before being damped completely, a narrow pseudogap forms near the Fermi level E_F. With further enhancement of g, there is a rapid shallowing of the pseudogap until finally a quasiparticle peak forms at E_F. At this stage, the system will have a Fermi-liquid character. Panel (c) represents a point in the Fermi-liquid metallic phase where, as explained below, the electron self-energy extrapolates to zero in the limit of $\omega_n \to 0$.

In the ED method, the virtual temperature $1/\tilde{\beta}$ plays the role of a lower-energy cutoff and ω_0 (the first Matsubara frequency) takes the value of $\pi/\tilde{\beta}$. In order to see whether or not the $\lim \Sigma(i\omega_0) \to 0$ as $\omega_0 \to 0$, we have used three different values for $\tilde{\beta}$ ($\tilde{\beta}=300, 400, 500$) or equivalently three different values for ω_0, and by way of extrapolating we have found that the limit of self-energy approaches zero. The choice of a finite number of bath levels, n_s, introduces a systematic error in the evaluation of $\mathrm{Im}\,\Sigma(i\omega_n)$, particularly at very low frequencies, and working with larger values of $\tilde{\beta}$ does not eliminate the above-mentioned systematic errors. This inherent inaccuracy restricts the precise evaluation of the range of non-Fermi-liquid behavior in the vicinity of g_{c1}. Our calculations, using different $\tilde{\beta}$ values, show that the inaccuracy at the critical e-ph coupling for the transition from the Kondo insulating phase to the non-Fermi metallic phase and from the non-Fermi metallic phase to the Fermi-liquid phase are at most equal to 0.02, thereby leaving the overall picture of our phase diagram nearly the same. For clarification purposes, we have shaded the non-Fermi-liquid region in Fig. 1. More detailed results on the spectra might be obtained by the numerical renormalization-group (NRG) technique.

Upon increasing g further, there is a weak narrowing of the quasiparticle peak until it disappears at the second critical value of e-ph coupling, g_{c2}, where a gap opens. The inset of panel (d) shows the double occupancy $d=\langle n_\uparrow n_\downarrow \rangle$ as a function of g. There is no signature of the Kondo insulator-metal transition in the double occupancy, but at g_{c2} the double occupancy jumps suddenly to $d \approx 1/2$, indicating a discontinuous transition to the bipolaronic phase.

The top panel of Fig. 3 shows the phonon spectral function, $\rho_{\mathrm{ph}}(\omega) = -\mathrm{Im}\, d(\omega + i0^+)/\pi$, for $J=0.1$ as a function of e-ph interaction strengths. The phonon Green's function is defined by $d(\omega) = \langle\langle b_i; b_i^\dagger \rangle\rangle_\omega$. There is no signature of the transition from the Kondo insulating phase to the metallic (non-Fermi) state in the phonon spectrum, whereas the transition from the metallic phase to the bipolaronic phase is clearly visible by the negative spectral weight. The justification for this is that in our model phonons couple to the charge fluctuations. The effect of an increasing g near g_{c1} is just to enhance the charge fluctuations continuously, resulting in a stronger coupling between electrons and phonons

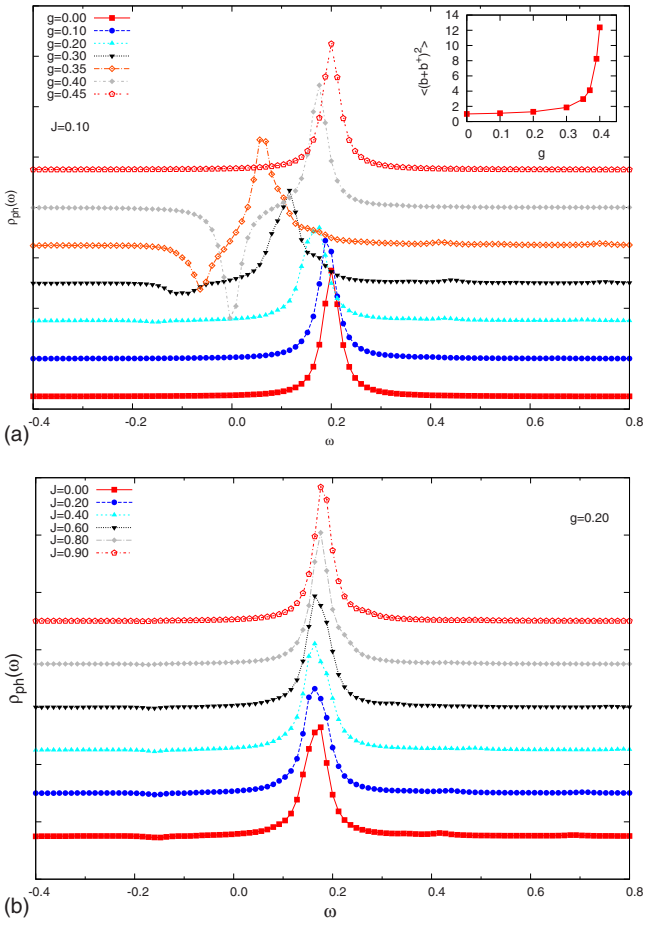

FIG. 3. (Color online) Phonon spectral function for different values of g. The bare phonon frequency is $\Omega_0=0.2$ and a Lorentzian broadening with the full width at half maximum of 0.02 has been implemented. Top panel: spectral function for $J=0.1$ and various values of g. A considerable phonon softening is seen upon approaching the transition to the bipolaronic insulator. The inset shows the expectation value of lattice fluctuations, $\langle(b+b^\dagger)^2\rangle$, as a function of the electron-phonon coupling g. Bottom panel: spectral function for $g=0.2$ and various values of J. The transition to Kondo insulator does not obviously affect the phonon spectral function.

which leads to the softening of the phonon. Our calculation of the phonon spectral function for the points in the non-Fermi-liquid region for different J values indicates that as long as we are away from the bipolaronic phase, the phonon spectral function appears just like the case shown in the top panel of Fig. 3, except that it is slightly shifted to the left and is somewhat widened.

The top panel of Fig. 3 also illustrates how the phonon mode is softened with increasing g. The softening phonon mode is a manifestation of a lattice instability similar to the structural phase transitions occurring in crystals. Stability is restored by the condensation of the unstable mode which is the result of a nonzero expectation value of the phonon operator ($\langle b \rangle \neq 0$) or in the large average number of excited phonons in the ground state (see the inset of the top panel of Fig. 3). The appearance of a negative spectral function for $\omega < 0$ when the bipolaronic state is approached implies that there is a large increase in the lattice displacement. In the

bipolaronic state, the phonon mode hardens back to the bare mode as g assumes values greater than g_{c2}. This is due to the fact that screening is not effective in an insulating state which is the same behavior already seen for the pure Holstein model.[24] The bottom panel of Fig. 3 shows the phonon spectral function for $g=0.2$ and various values of J. The phonon mode gradually hardens back to Ω_0, as the J values increase. We observe no signature of a transition to the Kondo insulator in the phonon spectrum. The effect of increasing J is to suppress continuously the charge fluctuations, which results in a decoupling of electrons and phonons, causing the phonon peak to exhibit hardening. In contrast to the Holstein-Hubbard model results, where softening is absent in the Mott insulator phase and phonons are effectively decoupled from electrons,[24] here the hardening of the phonon peak takes place very slowly.

IV. CONCLUDING REMARKS

In conclusion, we have studied the Holstein-Kondo lattice model at half filling which has been useful in the study of heavy-fermion semiconductors. We find that the model presents the physics of the Kondo insulator when the exchange coupling J plays a dominant role and a transition to correlated metal takes place for small J and intermediate e-ph coupling g. Moreover, a bipolaronic-metal insulator transition takes place for small J and large g. We also find a small region with non-Fermi-liquid character near the Kondo insulator-metal transition.

As mentioned in Sec. I, it has been shown experimentally that the heavy-fermion semiconductors exhibit a spin and a charge gap at low temperatures typically ranging from 1 to 100 meV.[1,2] Our phase diagram is consistent with these findings. A direct and quantitative comparison with the experimental values of these gaps requires accurate DOS calculations of a given system. However, since our model is solved by employing the DMFT in conjunction with the ED technique, we were not able to present a quantitative account of the above-mentioned gaps. To do so, one needs to use other techniques such as the NRG. Works in this direction are in progress.

Moreover, we and other researchers have studied the two-channel Kondo lattice model.[25,26] Extension of the present work to the Holstein–two-channel Kondo lattice model would shine light on the properties of the heavy-fermion systems.

The remaining interesting questions will be how the phase diagram and the nature of transitions will change as the vibrational frequency Ω_0 or electron density n is changed. It is also interesting to study the symmetry-breaking states such as the antiferromagnetic and superconducting states.

[1] P. S. Riseborough, Adv. Phys. **49**, 257 (2000).
[2] P. Mira, *Heavy-Fermion Systems* (Elusive, Amsterdam, 2008).
[3] M. Jaime, R. Movshovich, G. R. Stewart, W. P. Beyermann, M. G. Berisso, M. F. Hundley, P. C. Canfield, and J. L. Sarrao, Nature (London) **405**, 160 (2000).
[4] J. C. Cooley, C. H. Mielke, W. L. Hults, J. D. Goettee, M. M. Honold, R. M. Modler, A. Lacerda, D. G. Rickel, and J. L. Smith, J. Supercond. **12**, 171 (1999).
[5] M. Loewenhaupt, U. Witte, S. Kramp, M. Braden, and P. Svoboda, Physica B **312-313**, 181 (2002).
[6] S. Yotsuhashi, M. Kojima, H. Kusunose, and K. Miyake, J. Phys. Soc. Jpn. **74**, 49 (2005).
[7] T. Hotta, Phys. Rev. Lett. **96**, 197201 (2006).
[8] P. Nayak, B. Ojha, S. Mohanty, and S. N. Behera, Int. J. Mod. Phys. B **16**, 3595 (2002).
[9] K. S. Burch, E. E. M. Chia, D. Talbayev, B. C. Sales, D. Mandrus, A. J. Taylor, and R. D. Averitt, Phys. Rev. Lett. **100**, 026409 (2008); K. S. Burch, A. Schafgans, N. P. Butch, T. A. Sayles, M. B. Maple, B. C. Sales, D. Mandrus, and D. N. Basov, *ibid.* **95**, 046401 (2005).
[10] A. Georges, G. Kotlier, W. Kraut, and M. J. Rosenberg, Rev. Mod. Phys. **68**, 13 (1996).
[11] M. Caffarel and W. Krauth, Phys. Rev. Lett. **72**, 1545 (1994).
[12] All calculations presented in this paper are tested for $\tilde{\beta}=300,400$, and no visible difference in our numerical results is detected.
[13] G. Sangiovanni, M. Capone, and C. Castellani, Phys. Rev. B **73**, 165123 (2006).
[14] A. C. Hewson, *The Kondo Problem to Heavy Fermions*, Cambridge Studies in Magnetism (Cambridge University Press, Cambridge, 1997).
[15] S. Doniach, Physica B & C **91B**, 231 (1977).
[16] P. Werner and A. J. Millis, Phys. Rev. B **74**, 155107 (2006).
[17] T. A. Costi and N. Manini, J. Low Temp. Phys. **126**, 835 (2002).
[18] M. Capone and S. Ciuchi, Phys. Rev. Lett. **91**, 186405 (2003).
[19] W. Koller, D. Meyer, Y. Ono, and A. C. Hewson, Europhys. Lett. **66**, 559 (2004).
[20] G. S. Jeon, T. H. Park, J. H. Han, H. C. Lee, and H. Y. Choi, Phys. Rev. B **70**, 125114 (2004).
[21] D. Meyer, A. C. Hewson, and R. Bulla, Phys. Rev. Lett. **89**, 196401 (2002).
[22] M. Capone, G. Sangiovanni, C. Castellani, C. Di Castro, and M. Grilli, Phys. Rev. Lett. **92**, 106401 (2004).
[23] R. Pietig, R. Bulla, and S. Blawid, Phys. Rev. Lett. **82**, 4046 (1999).
[24] W. Koller, D. Meyer, and A. C. Hewson, Phys. Rev. B **70**, 155103 (2004).
[25] R. Nourafkan and N. Nafari, J. Phys.: Condens. Matter **20**, 255231 (2008).
[26] M. Jarrell, H. Pang, and D. L. Cox, Phys. Rev. Lett. **78**, 1996 (1997).